

Mutual information neural estimation in CNN-based end-to-end medical image registration

Yechong Huang^{1,2}, Tao Song², Jieru Zhu^{2,3}, Wenqi Luo¹, Jiahang Xu¹, Xiahai Zhuang^{1*}

¹School of Data Science, Fudan University, Shanghai, China

²SenseTime Technology, Shanghai, China

³Harbin Institute of Technology, Harbin, China

Corresponding author: Xiahai Zhuang, zxh@fudan.edu.cn

Abstract. Image registration is one of the most underlined processes in medical image analysis. Recently, convolutional neural networks (CNNs) have shown significant potential in both affine and deformable registration. However, the lack of voxel-wise ground truth challenges the training of an accurate CNN-based registration. In this work, we implement a CNN-based mutual information neural estimator for image registration that evaluates the registration outputs in an unsupervised manner. Based on the estimator, we propose an end-to-end registration framework, denoted as MIRegNet, to realize one-shot affine and deformable registration. Furthermore, we propose a weakly supervised network combining mutual information with the Dice similarity coefficients (DSC) loss. We employed a dataset consisting of 190 pairs of 3D pulmonary CT images for validation. Results showed that the MIRegNet obtained an average Dice score of 0.960 for registering the pulmonary images, and the Dice score was further improved to 0.963 when the DSC was included for a weakly supervised learning of image registration.

Keywords: Mutual Information, Registration, Deep Learning, Neural Network

1 Introduction

Image registration, the process that aligns two or more images of the same scene, is a fundamental preprocessing procedure in medical image analysis. For years, attempts have been taken to improve the performance of both affine and deformable registration. Recently, deep-learning based registration methods have shown great potentials thanks to their efficiency in time consuming and robustness against noise.

Several convolutional neural network (CNN) based image registration methods have been proposed. Miao *et al.* implemented CNN regression in rigid registration between X-ray and CT images [1]. Yang *et al.* applied encoder-decoder CNN in the prediction of LDDMM momentum-parameterization [2]. Balakrishnan *et al.* adopted a U-net-like structure to generate the dense deformation field in the registration [3]. Hu *et al.* introduced anatomical labels to the loss function for weakly supervised training of image registration [4], Sokooti *et al.* realized multi-scale deformable registration [5], and de Vos *et al.* proposed an end-to-end iterative framework that combined affine and deformable registration together [6]. Most of the published methods use unsupervised learning strategies, because the ground truths of the registration parameters are usually

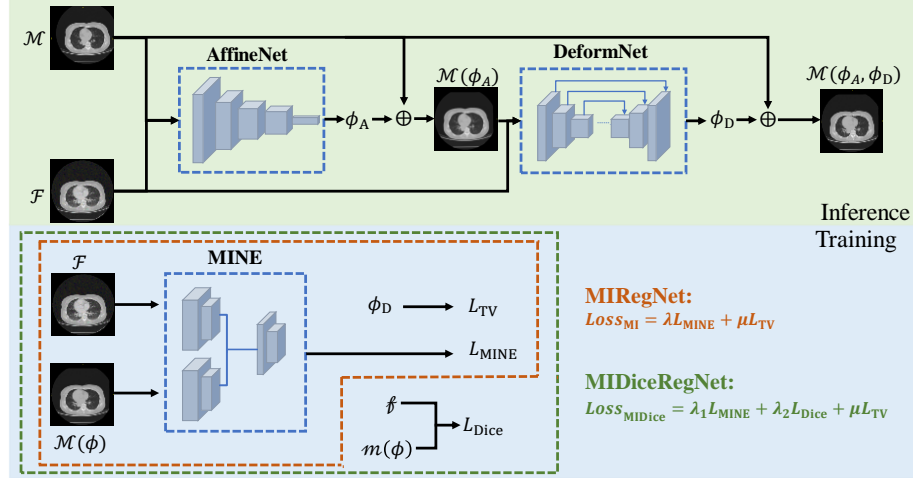


Figure 1 The overview of the proposed registration networks.

unavailable. As a result, a deep-learning based registration generally exploits convolution layers to aggregate multi-modality intensity features from the images and uses a similarity metric as the loss function to evaluate the results and back propagate the gradients.

However, calculating the similarity between two or more n -D images could be arduous. For example, mutual information (MI) is one of the most commonly used similarity metrics that quantifies the mutual dependencies [7]. MI has been proved to be credible in medical image registration over years [8, 9], but it requires the joint distribution of the voxel-wise intensities. Therefore, the direct implementation of the MI-based CNN can be challenging due to the difficulty of implementing efficient optimization with the back-propagation (BP) scheme. Recently, Belghazi *et al.* proposed a new idea of computing mutual information, based on an approximation using deep neural networks, i.e., the mutual information neural estimation (MINE) [10]. The effectiveness of the MINE has been validated in multiple tasks including autoencoders and generative adversarial networks. However, the extension of the MINE or the MI-based CNN for image registration has not been reported, to the best of our knowledge.

The main idea of the MINE is that the MI of two random variables is equivalent to the KL-divergence between the joint distribution and the product of the marginal distribution. The KL-divergence has a dual representation that is the upper bound of an objective function. As a result, the MINE converts the calculating of MI to the optimizing of an objective function, which is favorable for neural networks. Therefore, we propose to adopt the core idea of the MINE by using a CNN to represent the arguments of the objective function. By this means, one can calculate MI of the registration images and the derivative of MI via CNN efficiently. We refer to this registration CNN as the MIRegNet. Since only the fixed image and the moved image are needed for training, the MIRegNet is an unsupervised learning scheme. Furthermore, in many applications

one could obtain the segmentation masks of the object-of-interest for the training images. For these applications, we propose to include these mask images for a weakly supervised training of the registration networks. We adopt the Dice similarity coefficients (DSC) of the mask images, and combine the DSC as an auxiliary loss term with the MI loss. Hence, this network is referred to as MIDiceRegNet. We formulate both the affine and deformable registration. The smoothness regularization based on total variation (TV) of the displacement vector field (DVF) is included for the deformable registration. We employ the fully convolutional networks (FCN) and global average pooling (GAP) scheme in the sub-networks, and thus this framework is compatible on different image sizes.

2 Method

Figure 1 provides the overview of the proposed registration networks. We propose an end-to-end CNN-based registration framework that implements fast affine and deformable registration. Both of the MIRegNet and MIDiceRegNet consist two modules, i.e., the AffineNet for affine registration and the DeformNet for deformable registration.

2.1 Efficient Estimation of Mutual Information

Mutual Information(MI) is an effective metric which can represent the relationship between two random variables. It has been generally used to measure the similarity of paired images. It has the form as follows,

$$\begin{aligned} I(X; Y) &= \int_{\mathcal{X} \times \mathcal{Y}} \log \frac{d\mathbb{P}_{XY}}{d\mathbb{P}_X \otimes d\mathbb{P}_Y} d\mathbb{P}_{XY} \\ &= \mathbb{E}_{\mathbb{P}_{XY}} [\log (\frac{d\mathbb{P}_{XY}}{d\mathbb{P}_X \otimes d\mathbb{P}_Y})] = D_{KL}(\mathbb{P}_{XY} \parallel \mathbb{P}_X \otimes \mathbb{P}_Y), \end{aligned} \quad (1)$$

as X, Y represent two random variables, \mathbb{P}_{XY} denotes the joint distribution, $\mathbb{P}_X, \mathbb{P}_Y$ are the marginal distribution, $\mathbb{E}[\cdot]$ denotes the expectation, and D_{KL} denotes the KL-divergence. Calculating MI directly is costly and hard to back-propagate the derivative. Hence, we deduce a rapid approximation method according to the dual representation of the KL-divergence:

$$D_{KL}(\mathbb{P} \parallel \mathbb{Q}) = \sup_{T: \Omega \rightarrow \mathbb{R}} \mathbb{E}_{\mathbb{P}}[T] - \log(\mathbb{E}_{\mathbb{Q}}[e^T]), \quad (2)$$

where $T: \Omega \rightarrow \mathbb{R}$ represents all the mapping functions from the sample space Ω to a real number \mathbb{R} such that the two expectations are finite.

Considering the dual representation, one can efficiently obtain an approximation of MI by finding a appropriate T . Additionally, the mapping function has been proved to be able of being fit by a neural network. So we take advantage of MINE to improve the efficiency of registration. The application of MINE upon paired images could be depicted as:

$$I(\mathcal{M}; \mathcal{F}) = \sup_{\theta} \mathbb{E}_{\mathbb{P}_{\mathcal{MF}}} [T(\mathcal{M}, \mathcal{F}; \theta)] - \log(\mathbb{E}_{\mathbb{P}_{\mathcal{M}} \otimes \mathbb{P}_{\mathcal{F}}} [e^{T(\mathcal{M}, \mathcal{F}; \theta)}]), \quad (3)$$

where \mathcal{F} denotes the fixed image, \mathcal{M} denotes the moving image and θ denotes the MINE model parameters.

The joint distribution $\mathbb{P}_{\mathcal{MF}}$ could be represented by a well-designed two-entrance CNN, which takes \mathcal{F} and \mathcal{M} as input and concatenates the feature maps together. When calculating the product of the marginal distributions $\mathbb{P}_{\mathcal{M}} \otimes \mathbb{P}_{\mathcal{F}}$, we adopt to randomly shuffle the voxels of \mathcal{F} , denoted by $\tilde{\mathcal{F}}$. The shuffled image $\tilde{\mathcal{F}}$ has the same marginal distribution as \mathcal{F} , but is independent from \mathcal{M} . Therefore, $\mathbb{P}_{\mathcal{M}} \otimes \mathbb{P}_{\mathcal{F}}$ could be approximated by the joint distribution of $\tilde{\mathcal{F}}$ and \mathcal{M} that represented by CNN. We combine the representation of the joint distribution and the mapping function from the sample space to a real number together by adding convolution layers after the concatenated feature maps. The estimation of MI could be generated by finding a θ^* that maximizes the objective function, and the optimization of the objective function is implemented by the CNN optimizer and weighted back-propagation. Hence, the approximation of MI, between the fix image \mathcal{F} and the moving image $\mathcal{M}(\phi)$ by transformation ϕ , becomes equivalently to the following,

$$\begin{aligned} & I(\mathcal{M}(\phi); \mathcal{F}) \\ &= \sup_{\theta} \mathbb{E}[T_{\text{MINE}}(\mathcal{M}(\phi), \mathcal{F}; \theta)] - \log(\mathbb{E}[\exp(T_{\text{MINE}}(\mathcal{M}(\phi), \tilde{\mathcal{F}}; \theta))]) \quad (4) \\ &= \mathbb{E}[T_{\text{MINE}}(\mathcal{M}(\phi), \mathcal{F}; \theta^*)] - \log(\mathbb{E}[\exp(T_{\text{MINE}}(\mathcal{M}(\phi), \tilde{\mathcal{F}}; \theta^*))]). \end{aligned}$$

2.2 MIRegNet: An Unsupervised Registration Network

As shown in **Figure 1**, we propose an unsupervised end-to-end registration framework based on MINE, referred to as the MIRegNet, which consists of the AffineNet and the DeformNet.

In the inference, the AffineNet and the DeformNet implement registration in one-shot. The AffineNet adopts a spatial transformer network (STN) backbone, which takes the concatenation of the fixed image \mathcal{F} and the moving image \mathcal{M} as input, and generates a vector of affine parameters ϕ_A . The DeformNet is a variant of the U-net, as it uses encoding-decoding convolution layers and the skip connections to generate a displacement vector field (DVF) based on the \mathcal{F} and the affine-transformed moving image $\mathcal{M}(\phi_A)$. The generated DVF, ϕ_D , has the same image size of the $\mathcal{M}(\phi_A)$, but has three channels (ϕ^x, ϕ^y, ϕ^z) , as each channel represents the voxel-wise shifting of the corresponding coordinates. As a result, the moved image $\mathcal{M}(\phi_A, \phi_D)$ is generated by linear resampling.

In the training, MINE is used to estimate the MI between \mathcal{F} and $\mathcal{M}(\phi)$. For the deformable registration, we include the TV loss to obtain a smooth deformation field. TV represents the overall roughness of a DVF and is denoted by the L2-norm of the DVF divergence. Consequently, the loss function is defined as follows,

$$Loss_{MI} = \lambda \cdot L_{MINE} + \mu \cdot L_{TV}, \quad (5)$$

where, $L_{MINE}(\mathcal{M}(\phi); \mathcal{F}) = -I(\mathcal{M}(\phi); \mathcal{F})$ and $L_{TV}(\phi_D) = \|\nabla \phi_D\|^2$. The framework that adopts $Loss_{MI}$ is trained unsupervisedly, which is only based on MINE and the smoothness term.

2.3 MIDiceRegNet: A Weakly Supervised Registration Network

Furthermore, we introduce the Dice loss to the registration network when the segmentation labels are available from the training images. The anatomical labels do not directly imply the optimal registration parameters. However, they can be added as a constraint to the framework, and thus the framework is trained in a weakly supervised manner. Note that the anatomical labels, which are used to assist the training, are not involved in the inference. This registration network is denoted as the MIDiceRegNet.

Let \mathbf{f} and \mathbf{m} be the anatomical labels of \mathcal{F} and \mathcal{M} , respectively. In the training, the registration parameters ϕ are restored, and \mathbf{m} is transformed into a moved label $\mathbf{m}(\phi)$. The DSC between \mathbf{f} and $\mathbf{m}(\phi)$ is deduced as follows,

$$Dice(\mathbf{m}(\phi); \mathbf{f}) = \frac{2|\mathbf{m}(\phi) \cap \mathbf{f}|}{|\mathbf{m}(\phi)| + |\mathbf{f}|}. \quad (6)$$

Hence, the training loss of the MIDiceRegNet is defined as follows,

$$Loss_{MIDice} = \lambda_1 \cdot L_{MINE} + \lambda_2 \cdot L_{Dice} + \mu \cdot L_{TV}, \quad (7)$$

where $L_{Dice}(\mathcal{M}(\phi); \mathcal{F}) = -Dice(\mathbf{m}(\phi); \mathbf{f})$.

2.4 Training procedure

In both of the MIRegNet and the MIDiceRegNet, the AffineNet and the DeformNet are trained separately, as the outputs of the AffineNet are used as the training data of the DeformNet. Data augmentation methods, including shifting, padding, cropping and flipping, are employed to improve the generalization. We also adopt instance normalization, learning rate decay and weight decay to ensure the robustness and avoid overfitting. To compare these two loss functions, the network architecture and all the hyperparameters except λ are kept the same in the training, and the models that performed best in the validation set are restored to be further tested.

3 Experiment

3.1 Materials

A 3D pulmonary CT images dataset which was acquired from Tianjin Medical University Cancer Institute & Hospital is used for validation. For each participant, a CT scan without contrast and a CT scan with contrast were taken at the same time period, in

Table 1 Results of the registration. None indicates before registration. Paired t-test was used to evaluate the significance between the best method (bold font) and the other two methods: * for p-value < 0.05, ** for p-value < 0.01 and for *** p-value < 0.001.

Method	DSC	ASD/mm	HD/mm	Runtime/s
None	0.929 ± 0.028	2.39 ± 1.21	21.16 ± 13.4	-
Inter Observer	0.987 ± 0.006	0.42 ± 0.17	22.76 ± 7.25	-
ANTs	$0.944 \pm 0.030^{***}$	$0.92 \pm 0.58^{***}$	10.39 ± 6.27	707
MIRegNet	$0.960 \pm 0.009^{***}$	$0.70 \pm 0.17^{***}$	11.92 ± 6.94	14
MIDiceRegNet	0.963 ± 0.007	0.64 ± 0.13	$12.26 \pm 7.29^*$	14

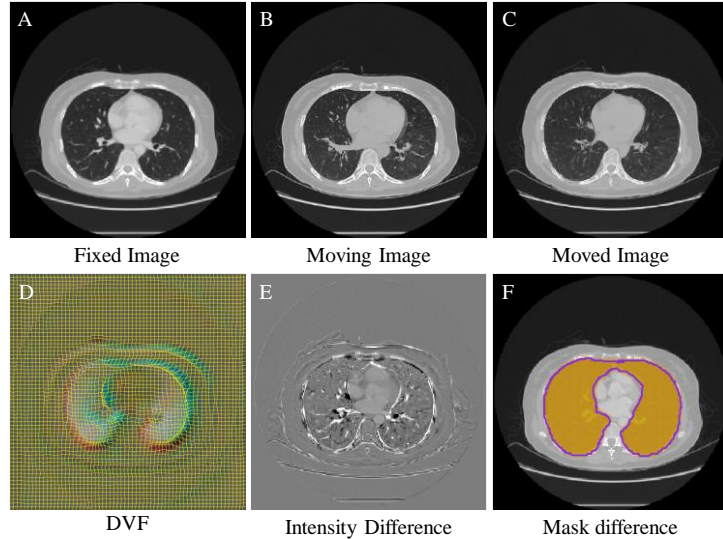


Figure 2 The result of the proposed framework trained by the MIDiceRegNet. Sub-figure D visualizes the DVF, figure E shows the voxel-wise intensity difference between fixed image and moved image, and figure F presents the difference between the segmentation mask of the fixed image and the wrapped mask of moved image.

which way a pair of CT images was obtained. Each CT image had an original size of $512 \times 512 \times 233$ with an original voxel spacing of $0.7812 \times 0.7812 \times 1.25$ mm. In the data pre-processing, we resampled and cropped each CT image into size of $320 \times 320 \times 320$ and voxel spacing of $1 \times 1 \times 1$ mm by linear interpolation. After resampling, the pulmonary parenchyma of each image was labelled. In total, 190 pairs of CT images and their segmentation were obtained. All the codes were written in Python. PyTorch was used to construct neural networks, and SimpleITK was used to process images. Advanced Normalization Tools (ANTs) was used to implemented conventional registration, as rigid registration, affine registration and symmetric registration was used [11].

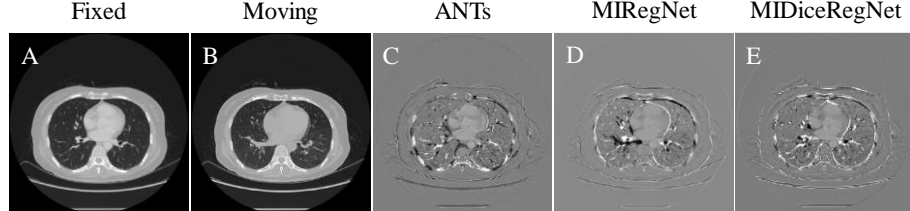


Figure 3 The difference image between the fixed image and the moved image registered by ANTs, MIRegNet and MIDiceRegNet.

3.2 Experimental Setup and Evaluation

The 190 paired CT images were randomly divided into a training set of 130 pairs, a validation set of 30 pairs and a test set of 30 pairs. In the framework, the CT images without contrast were used as the moving images while the CT images with contrast were used as the fixed images. To determine the balancing parameters of the loss function, we used 12 subjects of the training set, and obtained the parameters as, $\lambda = 1, \mu = 0.01$ for $Loss_{MI}$, and $\lambda_1 = \lambda_2 = 1, \mu = 0.01$ for $Loss_{MIDice}$.

To evaluate the registration accuracy, we calculated the DSC, the absolute surface distances (ASD) and the Hausdorff distances (HD) of the pulmonary parenchyma between the moved images and the fixed images. The computation time was also reported. For the test data, two experience observers were required to perform the manual labelling, and the inter-observer variation was then reported for reference.

3.3 Result and Discussion

Figure 2 demonstrates the outputs of the MIDiceRegNet. The proposed method realized high-quality voxel-wise image registration. **Figure 2D** visualizes the DVF generated by the MIDiceRegNet, which shows the main displacement occurs around the interface between the pulmonary parenchyma and other organs. **Figure 2E** shows the intensity difference between the fixed and moved images. One can see that the shapes of the pulmonary parenchyma and the cardiac chambers in two images are highly consistent, while the difference is mainly due to the costae and the trachea.

To further validate the proposed framework, we compared the result with conventional registration method, as listed in **Table 1**. MIRegNet and MIDiceRegNet achieved higher Dice scores than ANTs, the prevailing and certified conventional registration method. Lower absolute surface distances show that these two deep learning models generated high-quality smooth registration parameters. Besides, both of the two models realized the deformable registration in less than 15 seconds, much faster than ANTs. The deep learning-based methods showed great potentials of achieving better performed registration.

When taking usage of the anatomical labels, the method known as the MIDiceRegNet, the framework reached the best results. **Figure 3** further compares the registration

results given by ANTs, MIRegNet and MIDiceRegNet. MIDiceRegNet shows a clearer boundary of the pulmonary parenchyma. Besides, MIDiceRegNet and MIRegNet are more robust in the interface of the pulmonary parenchyma and the costae.

4 Conclusion

In this paper, we adopted the main idea of MINE, and extended its application to the medical image registration. Based on MINE, we proposed an end-to-end registration framework. This framework uses sequential AffineNet and DeformNet to generate the transformation parameters of both affine and deformable registration in one-shot. In the framework, MINE is used to estimate the MI between the fixed image and the moved image and back-propagate the training loss. The proposed MIRegNet is trained solely using the intensity information of the images, hence it is an unsupervised learning based method. Furthermore, we introduced a weakly-supervised learning method, i.e., MIDiceRegNet, where the DSC between segmentation masks is included into the training loss. Consequently, the MIDiceRegNet achieved better results than the unsupervised MIRegNet, though both of them outperformed the conventional method.

References

- [1] Miao, S., Wang, Z. J., Liao, R.: A CNN regression approach for real-time 2d/3d registration. *IEEE transactions on medical imaging* 35(5), pp. 1352-1363 (2016).
- [2] Xiao, Y., Kwitt, R., Niethammer, M.: Fast predictive image registration. *Deep Learning and Data Labeling for Medical Applications*, pp. 48-57 (2016).
- [3] Balakrishnan, G., Zhao, A., Sabuncu, M. R., Guttag, J., Dalca, A. V.: An unsupervised learning model for deformable medical image registration. *CVPR*, pp. 9252-9260 (2018).
- [4] Hu, Y., Marc, M., Eli, G., Wenqi, L., et al.: Weakly-supervised convolutional neural networks for multimodal image registration. *Medical image analysis* 49, pp. 1-13 (2018).
- [5] Sokooti, H., Vos, B. D., Berendsen, F., Lelieveldt, B. P. F., Isgum, I., Staring, M.: Nonrigid image registration using multi-scale 3D convolutional neural networks. *MICCAI*, pp. 232-239 (2017).
- [6] De Vos, B. D., Berendsen, F. F., Viergever, M. A., Sokooti, H., Staring, M., Isgum, I.: A deep learning framework for unsupervised affine and deformable image registration. *Medical Image Analysis* 52, pp. 128-143 (2019).
- [7] Viola, P., Wells, W. M.: Alignment by maximization of mutual information. *International journal of computer vision* 24(2), pp. 137-154 (1997).
- [8] Maes, F., Collignon, A., Vandermeulen, D., Marchal, G., Suetens, P.: Multimodality image registration by maximization of mutual information. *IEEE transactions on medical imaging* 16(2), pp. 187-198 (1997).
- [9] Pluim, J. P. W., Maintz, J., Viergever, M. A.: Mutual-information-based registration of medical images: a survey. *IEEE Trans on Med Imag* 22(8), pp. 986-1004 (2003).
- [10] Belghazi, M. I., Baratin, A., Rajeswar, S., Ozair, S., Bengio, Y., Courville, A., et al.: Mine: mutual information neural estimation. *arXiv preprint arXiv: 1801.04062* (2018).
- [11] Avants, B. B., Epstein, C. L., Grossman, M., Gee, J. C.: Symmetric diffeomorphic image registration with cross-correlation: evaluating automated labeling of elderly and neurodegenerative brain. *Medical image analysis* 12(1), pp. 26-41 (2008).